Changes in structure and dynamics of the Fv fragment of a catalytic antibody upon binding of inhibitor

GERARD J.A. KROON, HUAPING MO, MARIA A. MARTINEZ-YAMOUT, H. JANE DYSON, AND PETER E. WRIGHT

Department of Molecular Biology and Skaggs Institute of Chemical Biology, The Scripps Research Institute, La Jolla, California 92037, USA

(RECEIVED December 20, 2002; FINAL REVISION April 17, 2003; ACCEPTED April 18, 2003)

Abstract

Binding of the product inhibitor p-nitrophenol to the monoclonal esterolytic antibody NPN43C9 has been investigated by performing NMR spectroscopy of the heterodimeric variable-domain fragment (Fv) of the antibody in the presence and absence of inhibitor. Structural information from changes in chemical shift upon binding has been related to the changes in local dynamics in the active site of the catalytic antibody using NMR relaxation measurements. Significant changes in the chemical shifts of the backbone resonances upon binding extend beyond the immediate vicinity of the antigen binding site into the interface between the two associated polypeptides that form the Fv heterodimer, a possible indication that the binding of ligand causes a change in the relative orientations of the component light (V_L) and heavy (V_H) chain polypeptides. Significant differences in backbone dynamics were observed between the free Fv and the complex with p-nitrophenol. A number of resonances, including almost all of the third hypervariable loop of the light chain (L3), were greatly broadened in the free form of the protein. Other residues in the antigen-binding site showed less broadening of resonances, but still required exchange terms (R_{ex}) in the model-free dynamics analysis, consistent with motion on a slow timescale in the active site region of the free Fv. Binding of p-nitrophenol caused these resonances to sharpen, but some R_{ex} terms are still required in the analysis of the backbone dynamics. We conclude that the slow timescale motions in the antigen-binding site are very different in the bound and free forms of the Fv, presumably due to the damping of large-amplitude motions by the bound inhibitor.

Keywords: Catalysis; NMR; relaxation measurements; anisotropy; model-free analysis

A great deal of structural work, by both X-ray crystallography and NMR spectroscopy, has been focused on antibody combining sites. In particular, the structure of the combining site in the presence and absence of ligands has been examined in detail by X-ray crystallography, and it appears that the incidence of structural change upon ligand binding is quite variable. For example, the structures of some antibodies reveal significant changes in the antibody-binding site upon complexation (Stanfield et al. 1993), whereas more recent studies of catalytic antibodies with bound hapten reveal no major structural changes upon binding (Gigant et al. 1998; Thayer et al. 1999). The complementarity-determining regions (CDRs) of antibodies consist of loops of variable length which might well be intrinsically rather disordered. Because crystal packing can influence the conformation of these loops, it is of interest to examine the location and type of structural changes in solution, and to relate these to changes in the flexibility and dynamics of the complementarity-determining loops upon binding of ligands.

Reprint requests to: Peter E. Wright or H. Jane Dyson, Department of Molecular Biology, MB2, The Scripps Research Institute, 10550 N. Torrey Pines Road, La Jolla CA 92037, USA; e-mail: wright@scripps.edu or dyson@scripps.edu; fax: (858) 784-9822.

Article and publication are at http://www.proteinscience.org/cgi/doi/10.1110/ps.0243303.

Catalytic antibodies form a special class, where the specificity of antibody binding to ligands is utilized to catalyze a chemical or biochemical reaction. The thermodynamic and structural implications of this observation have been extensively discussed (Lerner et al. 1991; Schultz and Lerner 1993, 1995). Catalytic antibodies are generally raised against a strained transition state analog, and it appears that the specific binding energy of the antibody toward the immunogen can be harnessed in the analogous substrate to facilitate formation of the transition state. Catalytic antibodies generally show broader substrate specificity than natural enzymes and often have a lower turnover rate.

The catalytic monoclonal antibody NPN43C9 (Janda et al. 1988) is both an amidase and an esterase, catalyzing the hydrolysis of a variety of phenyl ester compounds and *p*-nitroanilides. Hydrolysis of the ester or amide bond is a multistep reaction that includes an acyl-antibody intermediate (Gibbs et al. 1992; Krebs et al. 1995). The rate-limiting step in the hydrolysis of the substrate *p*-nitrophenyl ester is the release of p-nitrophenol, for which the Fv has a strong affinity (K_d 0.6 μM; k_{off} 40 sec^{-1}; Gibbs et al. 1992). The structures of the original phosphonamidate immunogen, together with a representative substrate and the product inhibitor p-nitrophenol, are shown in Figure 1. The smallest portion of the NPN43C9 antibody molecule capable of catalysis is the ~25-kD variable fragment (Fv), which consists of a heterodimer of a 117-residue heavy chain variable region (V_H) and a 113-residue light chain variable region (V_L).

The three-dimensional structures of the Fv NPN43C9 and its binary complex with p-nitrophenol have been solved (Thayer et al. 1999). The nitrophenyl group is positioned in a deep pocket between the CDRs L1 and H3, making contact with residues His L91 and Tyr H95 (numbering according to Kabat et al. 1991). In the free form, the residues involved in the binding of p-nitrophenol form part of an extensive H-bond network with four water molecules. Mutations that disrupt this network cause changes in catalysis, which were interpreted as due to additional motion in the binding pocket (Thayer et al. 1999). To obtain insights into the intrinsic flexibility of the active site region of NPN43C9 and its possible role in catalysis, we have undertaken NMR relaxation experiments to probe directly the dynamics of the polypeptide backbone in both free and p-nitrophenol-bound states.

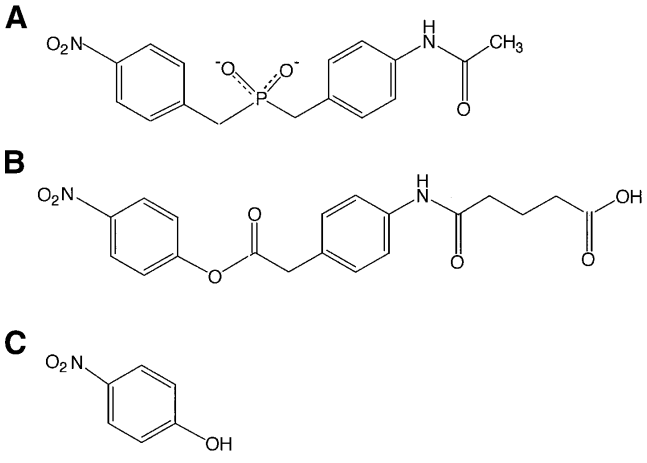

Figure 1. Structures of (*A*) the phosphoramidate immunogen used to elicit the antibody NPN43C9, (*B*) ester substrate of the catalytic antibody, and (*C*) product inhibitor p-nitrophenol.

Results

Preparation of ligand-free Fv

The final step in the purification of the catalytic Fv involves elution of the folded Fv heterodimer from an affinity column with excess p-nitrophenol. Because this yields the protein in complex with p-nitrophenol, a method had to be developed to remove the p-nitrophenol ligand from the Fv. This is not easy, as the protein must be maintained in its fully folded state during the process. Attempts to refold the protein from *E. coli* inclusion bodies showed that it cannot be reconstituted once it is unfolded. The high affinity of the p-nitrophenol makes it difficult to remove from the binding site without denaturation of the protein. Several methods, including elution of the protein from the affinity column at relatively low pH, gave samples of the free form that were prone to aggregation, presumably due to some local irreversible unfolding step. We were finally successful in obtaining stable samples of the free form by extensive dialysis of the purified p-nitrophenol complex, which resulted in complete removal of the p-nitrophenol ligand, according to UV absorbance measurements and HSQC NMR spectra. Samples prepared in this way were stable for a period of months.

Changes in chemical shifts upon binding of p-nitrophenol

Resonance assignments for the Fv bound to p-nitrophenol have been reported (Kroon et al. 1999). Backbone resonance assignments for the free Fv were made using ^{15}N NOESY-HSQC and ^{15}N TOCSY- HSQC spectra recorded at 800 MHz. Of the 219 backbone amides, 189 could be assigned for the free protein. The remaining resonances were absent from the spectrum, due either to rapid exchange with solvent, or to broadening of the resonance lines as a result of exchange processes on an intermediate timescale. The 22 unassigned residues in the V_H subunit are found in the first β-strand (Leu H4 to Ser H7), in and near CDR H1 (Leu H29, His H35, Trp H36, and Ser H40), in CDR H2 (Glu H58 and Tyr H59), in CDR H3 (Gly H96, Tyr H97,

Gly H99, and Ser H101), and in the region around CDR H3 (Tyr H90 to Val H93, Trp H103 to Gly H106). The eight unassigned residues in the V_L subunit are found near the N-terminus (Leu L2), in the third β-strand (Met L21), in CDR L1 (Leu L27B and Ala L34), in the fifth β-strand (Leu L47), in the seventh β-strand (Thr L69 and Ile L75), and in CDR L3 (Arg L96).

A comparison of a region of the $\{^1H\}$-^{15}N HSQC spectrum for the Fv in the presence and absence of p-nitrophenol is shown in Figure 2. It is clear that a number of resonances, not just those in the antigen-binding site, are shifted upon binding of ligand. The changes in chemical shifts of ^1H and ^{15}N for the backbone amides are plotted in Figure 3. Differences larger than 0.05 ppm for proton or larger than 0.5 ppm for nitrogen were observed for Asn L31 and Tyr L32 in CDR L1, Trp L35 and Tyr L36 immediately following CDR L1, Ala L51, Ser L52, and Ser L56 in CDR L2, Gln L90, Tyr L92, Ala L94, and Thr L97 in CDR L3, Tyr H32 in CDR H1, Asp H100 and Phe H100B in CDR H3, Ser H28 in the loop between the second and third β-strand, and Asn H73 in the loop between β-strands six and seven. The largest differences in chemical shifts are observed for the residues in CDR L3, with a maximum of 7.3 ppm for the ^{15}N chemical shift of Ala L94.

The locations of amide resonances that are perturbed upon binding of p-nitrophenol are shown in Figure 4, plotted on the backbone trace of the crystal structure (Thayer et al. 1999). All of the assigned residues in CDR L3 show significant changes in chemical shift upon binding of p-nitrophenol. Four residues at the C-terminal part of CDR L1 also show a substantial difference in chemical shift upon binding. Only four assigned residues in CDR H1 and CDR H3 are influenced by the binding of p-nitrophenol. Most of the residues showing changes are found in the V_L, suggesting that the position of the bound p-nitrophenol is closer to residues of the V_L than the V_H. The largest shifts are found in a part of the CDR L3 close to the residues involved in catalysis.

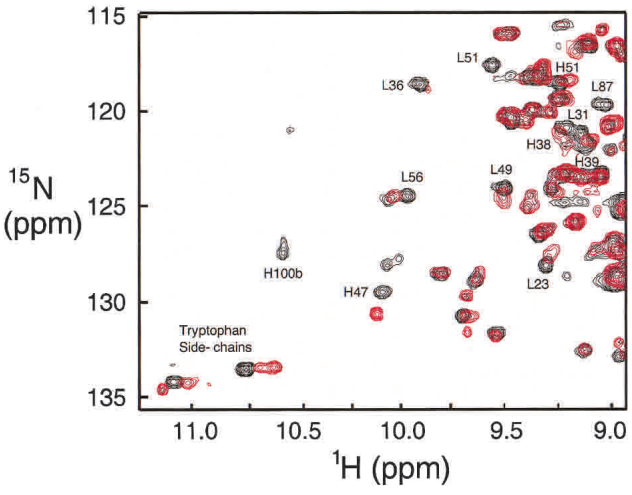

Figure 2. Comparison of a portion of the ^1H-^{15}N HSQC spectra of the Fv free and bound to the product inhibitor p-nitrophenol. Free Fv, red; p-nitrophenol complex, black.

No major changes in NOE patterns were observed for those residues that show large changes in chemical shifts when comparing data from the NOESY-HSQC spectrum of the free Fv fragment to that obtained for the p-nitrophenol complex. This indicates that the changes in chemical shifts are caused not by major structural changes but rather by changes in the local chemical environment.

Diffusion experiments

In order to determine the oligomerization state of the Fv, water-suppressed longitudinal encode-decode (water-sLED) experiments were performed (Altieri et al. 1995). The diffusion coefficients for the Fv in the presence and absence of p-nitrophenol were 0.97 and 0.95 × 10^{-6} cm^2s^{-1}, respectively. These results are midway between values of 1.08 and 0.82 × 10^{-6} cm^2s^{-1} obtained for lysozyme (14.1 kD) and IL-10 (37.2 kD), respectively (Altieri et al. 1995), consistent with the formation of a 25-kD heterodimer of the variable light chain V_L and variable heavy chain V_H in both the free and bound forms of the Fv. These measurements rule out dissociation of the Fv into monomers under the conditions of the NMR experiments, and show that further oligomerization does not occur.

Backbone relaxation measurements

Measurements of the T_1, T_2, and heteronuclear $\{^1H\}$-^{15}N NOE for the free Fv were made at 600 MHz, and those for the p-nitrophenol complex were made at 800 MHz. Figure 5 shows the values obtained for the V_H and V_L polypeptides of the free and bound forms of the Fv. Only well resolved cross-peaks in the ^{15}N HSQC were used in the analysis, due to the complications introduced by resonance overlap. Of the 189 assigned backbone amides in the free Fv, 10 were excluded because of severe overlap, and 31 residues were not observed in the heteronuclear NOE experiment. A total of 148 HN vectors were used in further analysis. In the p-nitrophenol complex, 171 backbone resonances were used in the analysis of the relaxation data. Of the 195 assigned amides, 17 were excluded because of severe overlap, and four were too weak for reliable analysis in the heteronuclear NOE experiments.

Diffusion tensor analysis

The inertia tensor for the free and bound forms of the Fv was calculated, based on the coordinates of the X-ray crystal

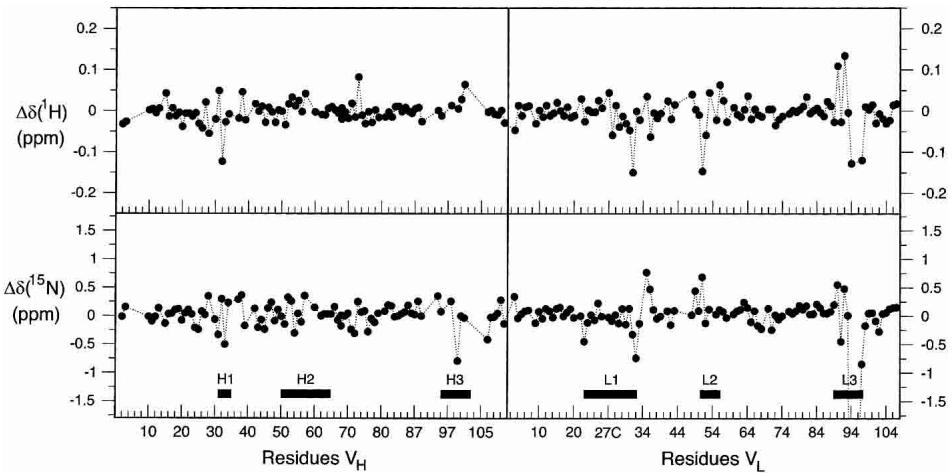

Figure 3. Plot of sequence locations of differences in amide chemical shift (free minus bound) between the free and p-nitrophenol-bound forms of the Fv. Value of $\Delta\delta(^{15}N)$ for residue 94 is 7.3 ppm.

structures of the free and bound Fv (Thayer et al. 1999). The values for the inertia tensor of both structures are 1.00 : 0.93 : 0.59, suggesting axial rotational anisotropy, which was accounted for in subsequent analysis of the backbone dynamics using ModelFree (Palmer 2000).

Before analysis of the diffusion tensor, residues with significant additional motions besides the overall tumbling must be eliminated. This was done using the method described by Tjandra et. al (1995), where residues with a heteronuclear NOE value lower than 0.65 were excluded, because this is an indication that these residues have high amplitude motions on a picosecond timescale.

After the first round of the diffusion tensor analysis for both the free Fv and the p-nitrophenol complex, some residues showed a poor fit in all three models (isotropic, axial, and anisotropic) resulting in a large value for χ^2 ($\chi^2 > 25$). The total χ^2 value for the diffusion tensor analysis decreased about 31% after removing residues Gly H26, Ala L12, Ser L14, and Ser L67 for the free Fv. Removing residues Ser H17, Lys H43, Gly H44, Ala L12, Ser L14, Ser L77, and Cys L88 for the p-nitrophenol complex resulted in a decrease of the total χ^2 value of 57%. For the free Fv (600 MHz), the relaxation data were fit best by $\tau_c = 12.3$ ns, $D_{\|}/D_{\perp} = 1.20$ and $\theta = 11.7°$ (θ is the angle between the principal axis of the diffusion tensor and the principal axis of the inertia tensor). The corresponding values for the inhibitor-bound Fv (800 MHz) are: $\tau_c = 13.9$ ns, $D_{\|}/D_{\perp} = 1.20$ and $\theta = 8.6°$.

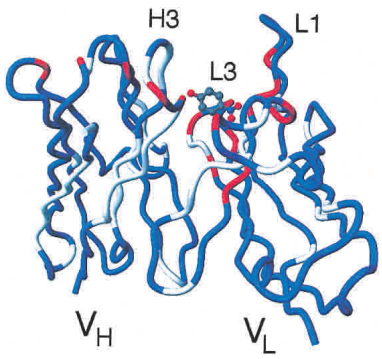

Figure 4. Locations of the amide proton and ^{15}N resonances that are perturbed upon complexation of p-nitrophenol, plotted onto the structure of p-nitrophenol-bound Fv (Thayer et al. 1999). Blue represents residues for which assignments could be made for both forms, and gray shows areas where resonances of the free and/or p-nitrophenol-bound forms could not be assigned. Red represents residues for which differences larger than 0.05 ppm for ^1H and/or larger than 0.5 ppm for ^{15}N were observed.

Model-free analysis

The results of the model-free analysis of the relaxation data are presented in Figure 6, and these values are mapped onto the structures of the free and bound Fvs in Figure 7. The S^2 values, which represent the nanosecond motions, indicate that the backbone of the protein is relatively rigid on a nsec timescale. The values do not differ greatly between the two forms of the protein. However, the τ_e (motion on a nsec timescale) and R_{ex} (motion on a μsec-msec timescale) terms show significant differences, and where they occur in the same positions for the two forms of the protein, may differ markedly in amplitude. It should be noted that the apparent significant increase in R_{ex} terms in the V_L domain upon binding of p-nitrophenol is somewhat misleading. The resonances of the CDR loop L3 are broadened in the free form of the protein, to such an extent that relaxation data cannot reliably be obtained for these regions of the protein. This broadness is most likely due to slow timescale motions. Upon binding of p-nitrophenol, these motions are damped, to the extent that the resonances are now sharp enough to be observed. Nevertheless, motion on a msec-μsec timescale

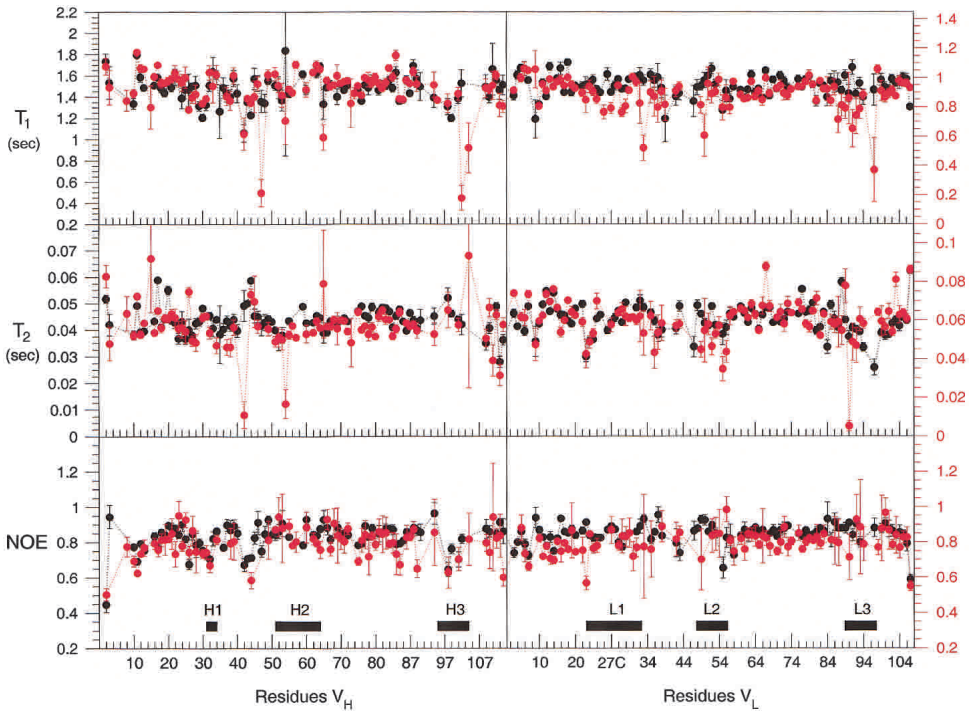

Figure 5. Per-residue plot of the T_1, T_2, and heteronuclear $\{^1H\}$-^{15}N NOEs measured for the Fv free (red) and in complex with p-nitrophenol (black). Axes labeled in black at the left of the figure refer to the 800 MHz data obtained for the Fv bound to p-nitrophenol. Axes labeled in red at the right of the figure refer to 600 MHz data obtained for the free Fv. The locations of the CDR loops on each chain of the heterodimer are indicated.

still occurs, giving rise to R_{ex} terms for the CDR loops in the bound form.

The model-free analysis of the Fv reveals the presence of different types of small-amplitude motions within local regions, even in the presence of a tightly bound inhibitor. Residues in the first loop close to the N-terminus of the V_H, between the first two β-strands (residues Gly H10 to Gln H16) of both the free and bound protein showed a combination of motions on both millisecond and picosecond timescales (see Fig. 6). Motions on a millisecond timescale were observed in three regions of the heavy chain of the free Fv (see Fig. 6). One of these regions, Gly H55 to Lys H64, is part of the CDR H2. The other two regions include the residues Gln H77 to Leu H80 and Leu H82C to Ala H91. In the CDR H1 from Ser H30 to Tyr H32, only motions on a picosecond timescale were observed. Residues in CDR H3 showed no additional motions. However, in this region no peaks were observed for residues Tyr H95, Gly H96, Tyr H97, Gly H99, Asp H100, Phe H100B, and Ser H101.

In the presence of bound p-nitrophenol, two regions with motions in the pico- to nanosecond timescale were observed for the heavy chain of the Fv. One region includes residues Gln H83 to Asp H85, and the second region comprises residues Gly H98, Gly H99, and Arg H100A, which are part of CDR H3. The light chain of the Fv with bound inhibitor contains two distinct regions with additional motions. The first region consisting of residues Val L3 to Thr L7 shows additional motions on a picosecond timescale. The second region consisting of residues Arg L93 to Lys L103 shows additional motions on a millisecond timescale. Residue Thr L97 shows the highest rate, 16 s^{-1}.

In the light chain of the free Fv, residues with additional motions are more scattered and no specific regions were observed (see Fig. 6). All observable residues in the three CDR regions of the V_L fitted to the simplest model. The residues Gln L89, His L91, Arg L96, and Thr L97 in the CDR L3 were too weak to be included in the model-free analysis.

Discussion

Evidence for intermediate exchange in parts of the free Fv

In both the free Fv and the p-nitrophenol complex, no signals were observed for any of the backbone amides of Leu H4 to Ser H7 in the first β-strand and those of Tyr H95 to Tyr H97 in the N-terminal part of CDR H3. These regions of the V_H are probably in intermediate exchange, and the lines are broadened beyond detection. There are no particular regions missing in the backbone assignments of the V_L.

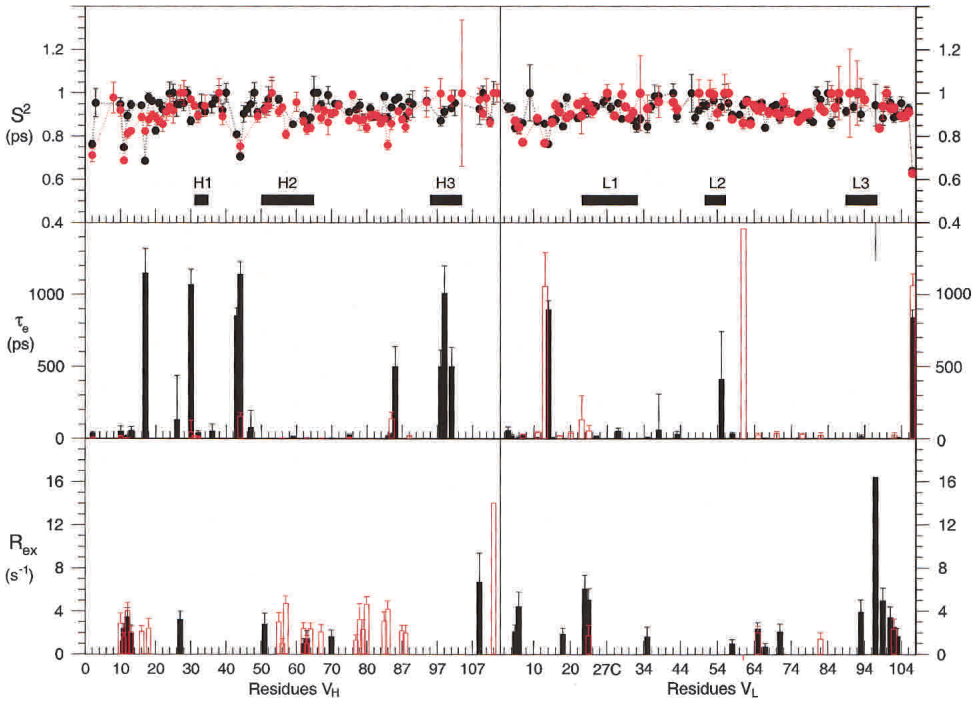

Figure 6. Calculated parameters S^2, τ_e, and R_{ex} from ModelFree 4.0 (Mandel et al. 1995) for the free (red) and p-nitrophenol-bound (black) Fv.

Similar observations were reported by Freund et al. (1994) in an NMR study of the Fv of the phosphorylcholine-binding antibody McPC603. Both the CDR H3 and CDR L3 were poorly defined due to a lack of information, whereas in our case only assignments for residues of the N-terminal part of the CDR H3 are missing.

Other evidence for motions in the same region of an antibody comes from X-ray crystallographic analysis of a catalytic Fab, where weak electron density due to disorder was seen for residues H98 to H100B in CDR H3 (Buchbinder et al. 1998). In contrast, the electron density maps for the crystal structure of antibody 43C9 are well resolved (Thayer et al. 1999). In this case, crystal packing effects may restrict motions of the CDRs that are visible in solution.

Dynamics of the Fv

The model-free analysis of the free Fv shows differences in the dynamical properties between V_L and V_H. Compared to the light chain, the heavy chain contains more residues that fit to a model with additional motions on a millisecond timescale. The difference between the two monomers is especially noticeable when comparing the CDRs. In the V_L, almost all observable residues in the CDRs fitted to the simplest model without any additional motions. Most of the observed residues in CDR H1 and H2 show additional mo-

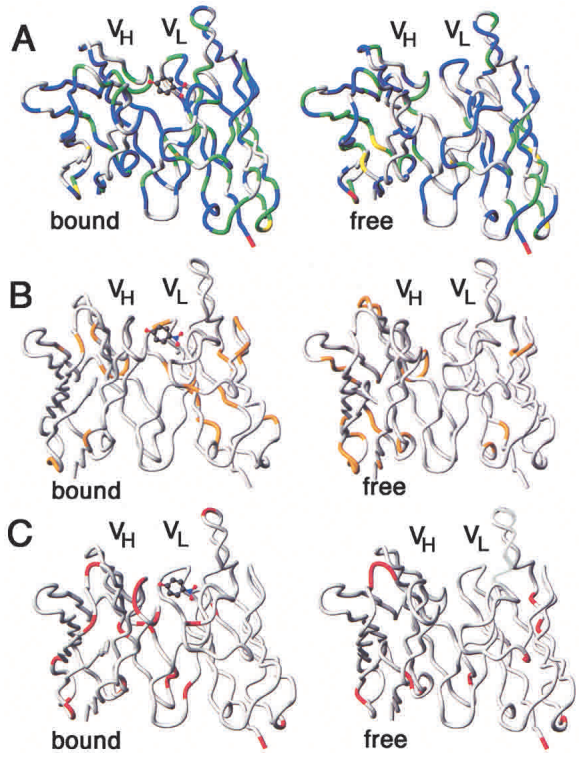

Figure 7. Mapping of model-free parameters onto structures of the free (*right* column) and p-nitrophenol-bound (*left* column) Fv (Thayer et al. 1999). (*A*) S^2 (red, $S^2 < 0.7$; yellow, $0.7 < S^2 < 0.8$; green, $0.8 < S^2 < 0.9$; blue, $S^2 > 0.9$). (*B*) $\tau_e > 50$ psec (orange) (*C*) R_{ex} (red).

tions on the picosecond and millisecond timescale, whereas all observed residues in CDR H3 show no additional motions. Despite the observed motions on the picosecond and millisecond timescale in both the V_L and V_H of the free Fv, the amplitudes of these motions are relatively small, as indicated by an overall large value for S^2 ($S^2 > 0.8$). One reason for the relative rigidity of the heterodimer could be explained by the formation of hydrogen bonds in the free Fv between residues of CDR H3 and L2 and between residues of CDR H2 and L3 (Thayer et al. 1999). The relatively high S^2 values for most of the residues analyzed in the Fv dimer indicates that the amplitude of motions in the backbone is limited. Residues of the loop regions of Gly H10 to Ala H13, Ser H40 to Gly H44, and Gln H83 to Asp H86 of the Fv in the p-nitrophenol complex show additional effective correlation times for internal motions on a picosecond to nanosecond timescale and additional dynamics on a microsecond to millisecond timescale. Residues in the C-terminal part of CDR L3 and the N-terminal part of the last β-strand in the p-nitrophenol complex have high exchange rates (Figs. 6,7). In the free Fv, these residues fit to the simplest model without any additional motions. The k_{off} rate constant for PNP is 40 s^{-1}, which is too slow to account for the R_{ex} terms observed in the bound form for these residues.

The only other relaxation data that have been reported for a complete Fv fragment are the heteronuclear NOE data on the phosphorylcholine-binding antibody McPC603 (Freund et al. 1994). No high-amplitude fast motions were observed in either the V_H or V_L, which is in good agreement with our results for the Fv 43C9. In the backbone dynamics study on the V_L domain of the Fv fragment of an antidigoxin antibody (26–10 V_L; Constantine et al. 1993), relatively high values for S^2 were found, in good agreement with the values calculated for the V_L domain of the NPN43C9 Fv. Of the 89 residues that were analyzed, 30 residues needed an additional exchange term in order to fit the relaxation data. Of the 67 residues of the free Fv 43C9, only four residues showed an additional R_{ex} term. The large number of residues with R_{ex} terms in the 26–10 V_L is most likely the result of neglecting to calculate the parameters by fitting to an anisotropic model, as we have done for the 43C9 Fv. However, some of the regions of the 26–10 monomer that display R_{ex} terms correspond to residues in the V_L domain of the p-nitrophenol complex of Fv NPN43C9 that undergo μsec-msec time scale motions. These residues are located in the N-terminal part of the V_L, the N-terminal part of CDR L1, and in the C-terminal part of CDR L3 (Fig. 7B).

Correlation of structural and dynamic changes upon ligand binding

Lindner et al. (1999) presented kinetic data for three catalytic antibodies with esterase activity that do not show the same severe product inhibition as the 43C9 antibody. These data suggest that some conformational flexibility provides an improved turnover rate through a mechanism termed "conformational isomerization" (Foote and Milstein 1994; Martinez-Yamout and McConnell 1994). The hypothesis is that there are multiple conformations of the antibody with different catalytic rates at pre-equilibrium, but during the catalysis only the most active conformation is retained.

In the case of Fv NPN43C9, no splitting of resonances was observed in the HSQC spectrum of the free form or the p-nitrophenol complex, indicating that multiple backbone conformations that interconvert slowly on the chemical shift timescale are absent. The NOE patterns observed in the ^{15}N NOESY spectra of the free and bound forms of the Fv show no differences, indicating that there are no major conformational changes upon binding. If conformational isomerization is part of the catalytic process for this antibody, it must be on a fast timescale, or else it must involve only side-chain rearrangements, which are not observed in the ^{15}N NOESY spectrum.

Residues Gln L89 to Thr L97 in the CDR L3 show the largest changes in chemical shift differences upon binding. These residues also show a significant change in the dynamics on a microsecond to millisecond timescale. In the free Fv, most of these residues were not observed in the T_2 experiment and the heteronuclear NOE experiment because of the extensive line-broadening. In the p-nitrophenol complex, these residues still have more than average line-broadening but less than for the free form. This observation is an indication that the motions of the backbone in this region become more restricted upon binding of the p-nitrophenol.

Are dynamics important in catalysis by antibodies?

It is clear that the CDR loops, which form the catalytic sites of catalytic antibodies, are mobile in the absence of substrate or inhibitor and that these regions acquire more complex motions on a slower timescale upon ligand binding. It has been suggested (Cannon and Benkovic 1998; Miller and Benkovic 1998; Bruice and Benkovic 2000) that microsecond-millisecond time scale motions could be coupled to the catalytic mechanisms of enzymes, and an apparent connection has been made in the case of DHFR (Radkiewicz and Brooks 2000; Agarwal et al. 2002). For the NPN43C9 Fv, a difference is observed in the μsec-msec timescale motion in the CDR loops upon binding of inhibitor, which could be interpreted as indicating connection between polypeptide chain motions and catalysis in this system. Analysis of the X-ray structures of the free and bound Fv (Thayer et al. 1999) reveals a possible mechanism for this coupling.

Mutation of arginine H100A to a glutamine decreased the p-nitrophenol binding and increased the catalytic rate at high pH. This residue lies outside the binding pocket in the X-ray structure, and it was suggested that its effect on catalysis is due to the presence of a hydrogen bond between

Arg H100A and the backbone of CDR H3 (Thayer et al. 1999). Loss of this hydrogen bond could increase the flexibility of the region, allowing more rapid loss of p-nitrophenol, and resulting in the increase in rate.

Coupling of polypeptide chain motion to catalysis remains an interesting hypothesis, which may be operative in certain enzymatic reactions, though probably not in all. Further investigation will be required to establish such connections unequivocally.

Materials and methods

Protein preparation

Protein samples uniformly labeled with ^{15}N were used in the NMR experiments. The protein was overexpressed in *Escherichia coli* and isolated as described (Kroon et al. 1999). To obtain the free Fv, half of the purified Fv was taken after purification and dialyzed for 14 d against a total 28 L buffer containing 10 mM Tris and 100 mM NaCl at pH6.8 at 4°C.

The NMR samples were concentrated and exchanged into 10 mM d_{11} Tris, 100 mM NaCl at pH6.8 using an Amicon Centriprep membrane filter with a 3-kD cutoff. To the sample containing the complex, additional p-nitrophenol was added to obtain a final concentration of 80 μM. The final protein concentration in the NMR samples of the free Fv and the p-nitrophenol complex was 0.5 mM as determined from the A_{280} absorption (extinction coefficient 48,000 M^{-1} cm^{-1}).

NMR experiments

The ^{15}N-labeled samples of both the free Fv and the p-nitrophenol complex were used to collect ^{1}H-^{15}N HSQC, ^{1}H-^{15}N NOESY-HSQC, and ^{1}H-^{15}N TOCSY-HSQC spectra on a Bruker DRX-800 spectrometer. Both 3D data sets consist of $1024*(t_1) \times 256*(t_2) \times 128*(t_3)$ data points. The experiments were collected with a spectral width of 7183.908 Hz (^{1}H), 11904.762 Hz (^{1}H), and 3846.154 Hz (^{15}N) and the carrier at 8.4 ppm, 4.70 ppm, and 119.4 ppm, respectively. The mixing times were 100 msec in the NOESY and 35 msec in the TOCSY experiment. The 2D ^{15}N HSQC on both samples were acquired with $2048*(t_1) \times 128*(t_2)$ using a spectral width of 7183.908 Hz (^{1}H) and 3846.154 Hz (^{15}N) and the carrier at 8.4 ppm and 120.9 ppm, respectively. Water suppression was achieved using the WATERGATE (Piotto et al. 1992) in combination with water flip-back pulses (Grzesiek and Bax 1993).

The T_1 and T_2 relaxation data and steady-state heteronuclear ^{15}N NOE data were recorded on Bruker DRX-600 and DRX-800 spectrometers, using the sensitivity-enhanced experiments described by Farrow et al. (1994). Water suppression was achieved using water flip-back pulses (Grzesiek and Bax 1993). All NMR relaxation experiments were recorded at 25.1°C calibrated using methanol. All relaxation data sets were acquired with $1024*(t_1) \times 256*(t_2)$ data points and a spectral width of 4807.692 Hz (^{1}H) and 2190.1011 Hz (^{15}N), respectively. The carrier was set at 7.52 ppm (^{1}H) and 118.8 ppm (^{15}N). The same sample used for the backbone assignments of the free Fv was also used in the relaxation experiments.

The T_1 relaxation rate was sampled using 10 different timepoints: 10, 80 (2x), 160, 1200, 520 (2x), 880, 2000 (2x), 3000, 4000, and 6000 msec for both the free Fv and the p-nitrophenol complex at 600 MHz. The T_2 relaxation rate was sampled using 8 different timepoints: 6, 18, 34, 68 (2x), 106, 154 (2x), 210, and 322 msec for both the free Fv and the p-nitrophenol complex at 600 MHz. Data at the different time points in both T_1 and T_2 experiments were acquired in a random order to avoid systematic errors. For both samples, three sets of the steady-state ^{15}N heteronuclear NOE experiments were recorded, and for each set the saturated and unsaturated data were collected in an interleaved manner.

Spectra were processed using NMRpipe/NMRDRAW (Delaglio et al. 1995) and analyzed using NMRVIEW (Johnson and Blevins 1994) on a Silicon Graphics O2 workstation.

Relaxation data analysis

The T_1 and T_2 values for each residue were determined using the Curvefit program (Mandel et al. 1995). Because all experiments sampled the full decay of the signals, a three-parameter fit was used on both the T_1 and T_2 curves. Overlapping peaks were not used in the analysis.

The relaxation data were used to determine the diffusion tensor using the crystal structures of the scFv and the scFv with bound p-nitrophenol (Thayer et al. 1999) and the quadric_diffusion program (Lee et al. 1997). Validation of the diffusion tensor calculation was performed using the program COPED (Osborne and Wright 2001). In order to exclude residues which show additional motions on a picosecond or millisecond timescale, a selection filter was applied prior to the diffusion tensor analysis (Tjandra et al. 1996).

Model-free analysis

The relaxation data were fit using the Model-free4.0 program (Mandel et al. 1995). This program is based upon the model-free formalism (Lipari and Szabo 1982a,b; Clore et al. 1990) and uses the correlation between relaxation rates and spectral density functions as described by Abragam (1961). During the analysis, the nitrogen-hydrogen bond length was set to 1.02 Å and the chemical shift anisotropy for the ^{15}N nucleus was set to −170.0 ppm (Tjandra et al. 1996). A total of five different models were used during the analysis (S^2, $S^2+\tau_e$, S^2+R_{ex}, $S^2+\tau_e+R_{ex}$, and $S^2{}_s+S^2{}_f+\tau_e$) as described by Mandel et al. 1995. The goodness of fit was determined by the value of the $\chi 2$ function with a critical value of $\alpha = 0.05$. An F-test was applied with a critical value of $\alpha = 0.15$ to decide whether the improvement of a fit using an extended model was statistically valid.

Diffusion experiments

The self-diffusion (D_s) coefficient for the free Fv and the Fv with p-nitrophenol was determined using a series of 1D water-sLED experiments (Altieri et al. 1995) with different gradient strengths (6.8, 8.9, 10.9, 12.9, 14.9, 17.0, 19.0, 21.0, 23.0, 25.0, and 27.1 G/cm). The values of D_s for the different Fv samples were compared to that determined for a 2-mM lysozyme sample, as well as with literature values (Altieri et al. 1995). The experiments were performed on a Bruker DRX-600 spectrometer at 25°C using the same Fv samples used in the relaxation experiments.

Acknowledgments

We thank Professor Stephen Benkovic for numerous helpful discussions, and for providing the original clone for the NPN43C9 Fv; Drs. Brendan Duggan, Ishwar Radhakrishnan, Michael Os-

borne, John Viles, James Huntley, Brian Lee, and Eduardo Zaborowski for helpful discussions and for making available programs and scripts; John Chung for help with NMR spectrometer setup; and Linda Tennant for technical assistance. This work was supported by grant CA 27489 from the NIH.

The publication costs of this article were defrayed in part by payment of page charges. This article must therefore be hereby marked "advertisement" in accordance with 18 USC section 1734 solely to indicate this fact.

References

Abragam, A. 1961. *Principles of nuclear magnetism*, Clarendon Press, Oxford.

Agarwal, P.K., Billeter, S.R., Rajagopalan, P.T.R., Benkovic, S.J., and Hammes-Schiffer, S. 2002. Network of coupled promoting motions in enzyme catalysis. *Proc. Natl. Acad. Sci.* **99:** 2794–2799.

Altieri, A.S., Hinton, D.P., and Byrd, R.A. 1995. Association of biomolecular systems via pulsed field gradient NMR self-diffusion measurements. *J. Am. Chem. Soc.* **117:** 7566–7567.

Bruice, T.C. and Benkovic, S.J. 2000. Chemical basis for enzyme catalysis. *Biochemistry* **39:** 6267–6274.

Buchbinder, J.L., Stephenson, R.C., Scanlan, T.S., and Fletterick, R.J. 1998. A comparison of the crystallographic structures of two catalytic antibodies with esterase activity. *J. Mol. Biol.* **282:** 1033–1041.

Cannon, W.R. and Benkovic, S.J. 1998. Solvation, reorganization energy, and biological catalysis. *J. Biol. Chem.* **273:** 26257–26260.

Clore, G.M., Szabo, A., Bax, A., Kay, L.E., Driscoll, P.C., and Gronenborn, A.M. 1990. Deviations from the simple two-parameter model-free approach to the interpretation of nitrogen-15 nuclear magnetic relaxation of proteins. *J. Am. Chem. Soc.* **112:** 4989–4991.

Constantine, K.L., Friedrichs, M.S., Goldfarb, V., Jeffrey, P.D., Sheriff, S., and Mueller, L. 1993. Characterization of the backbone dynamics of an antidigoxin antibody V_L domain by inverse detected ^{1}H-^{15}N NMR: Comparisons with X-ray data for the fab. *Proteins* **15:** 290–311.

Delaglio, F., Grzesiek, S., Vuister, G.W., Guang, Z., Pfeifer, J., and Bax, A. 1995. NMRPipe: A multidimensional spectral processing system based on UNIX pipes. *J. Biomol. NMR* **6:** 277–293.

Farrow, N.A., Muhandiram, R., Singer, A.U., Pascal, S.M., Kay, C.M., Gish, G., Shoelson, S.E., Pawson, T., Forman-Kay, J.D., and Kay, L.E. 1994. Backbone dynamics of a free and a phosphopeptide-complexed Src homology 2 domain studied by ^{15}N NMR relaxation. *Biochemistry* **33:** 5984–6003.

Foote, J. and Milstein, C. 1994. Conformational isomerism and the diversity of antibodies. *Proc. Natl. Acad. Sci.* **91:** 10370–10374.

Freund, C., Ross, A., Plückthun, A., and Holak, T.A. 1994. Structural and dynamic properties of the F_v fragment and the single-chain F_v fragment of an antibody in solution investigated by heteronuclear three-dimensional NMR spectroscopy. *Biochemistry* **33:** 3296–3303.

Gibbs, R.A., Benkovic, P.A., Janda, K.D., Lerner, R.A., and Benkovic, S.J. 1992. Substituent effects on an antibody-catalyzed hydrolysis of phenyl esters: Further evidence for an acyl-antibody intermediate. *J. Am. Chem. Soc.* **114:** 3528–3534.

Gigant, B., Charbonnier, J., Eshhar, Z., Green, B.S., and Knossow, M. 1998. Crossreactivity, efficiency and catalytic specificity of an esterase-like antibody. *J. Mol. Biol.* **284:** 741–750.

Grzesiek, S. and Bax, A. 1993. The importance of not saturating H_2O in protein NMR. Application to sensitivity enhancement and NOE measurements. *J. Am. Chem. Soc.* **115:** 12593–12594.

Janda, K.D., Schloeder, D., Benkovic, S.J., and Lerner, R.A. 1988. Induction of an antibody that catalyzes the hydrolysis of an amide bond. *Science* **241:** 1188–1191.

Johnson, B.A. and Blevins, R.A. 1994. NMRView: A computer program for the visualization and analysis of NMR data. *J. Biomol. NMR* **4:** 604–613.

Kabat, E.A., Wu, T.T., Perry, H.M., Gottesman, K.S., and Foeller, C. 1991. *Sequences of proteins of immunological interest*, National Institutes of Health, Bethesda, MD.

Krebs, J.F., Siuzdak, G., Dyson, H.J., Stewart, J.D., and Benkovic, S.J. 1995. Detection of a catalytic antibody species acylated at the active site by electrospray mass spectrometry. *Biochemistry* **34:** 720–723.

Kroon, G.J.A., Martinez-Yamout, M.A., Krebs, J.F., Chung, J., Dyson, H.J., and Wright, P.E. 1999. Backbone resonance assignments for the Fv fragment of the catalytic antibody NPN43C9 with bound *p*-nitrophenol. *J. Biomol. NMR* **15:** 83–84.

Lee, L.K., Rance, M., Chazin, W.J., and Palmer, A.G. 1997. Rotational diffusion anisotropy of proteins from simultaneous analysis of ^{15}N and ^{13}C α nuclear spin relaxation. *J. Biomol. NMR.* **9:** 287–298.

Lerner, R.A., Benkovic, S.J., and Schultz, P.G. 1991. At the crossroads of chemistry and immunology: Catalytic antibodies. *Science* **252:** 659–667.

Lindner, A.B., Eshhar, Z., and Tawfik, D.S. 1999. Conformational changes affect binding and catalysis by ester-hydrolysing antibodies. *J. Mol. Biol.* **285:** 421–430.

Lipari, G. and Szabo, A. 1982a. Model-free approach to the interpretation of nuclear magnetic resonance relaxation in macromolecules. 1. Theory and range of validity. *J. Am. Chem. Soc.* **104:** 4546–4559.

———. 1982b. Model-free approach to the interpretation of nuclear magnetic resonance relaxation in macromolecules. 2. Analysis of experimental results. *J. Am. Chem. Soc.* **104:** 4559–4570.

Mandel, A.M., Akke, M., and Palmer, A.G. 1995. Backbone dynamics of *Escherichia coli* ribonuclease HI: Correlations with structure and function in an active enzyme. *J. Mol. Biol.* **246:** 144–163.

Martinez-Yamout, M. and McConnell, H.M. 1994. Site-directed mutagenesis and ^{1}H nuclear magnetic resonance of an antidinitrophenyl spin label antibody. *J. Mol. Biol.* **244:** 301–318.

Miller, G.P. and Benkovic, S.J. 1998. Stretching exercises—Flexibility in dihydrofolate reductase catalysis. *Chem. Biol.* **5:** 105–113.

Osborne, M.J. and Wright, P.E. 2001. Anisotropic rotational diffusion in model-free analysis for a ternary-DHFR complex. *J. Biomol. NMR* **19:** 209–230.

Palmer, A.G. 2000. ModelFree 4.10. http://cpmcnet.columbia.edu/dept/gsas/biochem/labs/palmer/software.html

Piotto, M., Saudek, V., and Sklenár, V. 1992. Gradient-tailored excitation for single-quantum NMR spectroscopy of aqueous solutions. *J. Biomol. NMR* **2:** 661–665.

Radkiewicz, J.L. and Brooks III, C.L. 2000. Protein dynamics in enzymatic catalysis: Exploration of dihydrofolate reductase. *J. Am. Chem. Soc.* **122:** 225–231.

Schultz, P.G. and Lerner, R.A. 1993. Antibody catalysis of difficult chemical transformations. *Accounts Chem. Res.* **26:** 391–395.

———. 1995. From molecular diversity to catalysis: Lessons from the immune system. *Science* **269:** 1835–1842.

Stanfield, R.L., Takimoto-Kamimura, M., Rini, J.M., Profy, A.T., and Wilson, I.A. 1993. Major antigen-induced domain rearrangements in an antibody. *Structure* **1:** 83–93.

Thayer, M.M., Olender, E.H., Arvai, A.S., Koike, C.K., Canestrelli, I.L., Stewart, J.D., Benkovic, S.J., Getzoff, E.D., and Roberts, V.A. 1999. Structural basis for amide hydrolysis catalyzed by the 43C9 antibody. *J. Mol. Biol.* **291:** 329–345.

Tjandra, N., Feller, S.E., Pastor, R.W., and Bax, A. 1995. Rotational diffusion anisotropy of human ubiquitin from ^{15}N NMR relaxation. *J. Am. Chem. Soc.* **117:** 12562–12566.

Tjandra, N., Szabo, A., and Bax, A. 1996. Protein backbone dynamics and ^{15}N chemical shift anisotropy from quantitative measurement of relaxation interference effects. *J. Am. Chem. Soc.* **118:** 6986–6991.